Slow-Burn Ammonium Perchlorate Propellants with Oxamide: Burn Rate Model, Testing, and Applications

Slow-burn ammonium perchlorate composite propellants with oxamide: burn rate model, testing and applications

Matthew T. Vernacchia*, Kelly J. Mathesius† and R. John Hansman‡
Massachusetts Institute of Technology, Cambridge, Massachusetts, 02139

Low-thrust, long-burn-time solid rocket motors may be useful as propulsion for small, fast uncrewed aerial vehicles. These motors require a slow-burning propellant which can operate at unusually low chamber pressures (0.3–2 MPa). Slow-burn propellants were developed using ammonium perchlorate oxidizer and the burn rate suppressant oxamide. By varying the amount of oxamide (from 0-20%), burn rates from $4\,\mathrm{mm\,s^{-1}}$ to $1\,\mathrm{mm\,s^{-1}}$ (at 1 MPa) were achieved. The adjustable burn rate allows a set of similar propellants to serve many aircraft and mission concepts. This work presents burn rate measurements (from both a strand burner and a research motor), minimum burn pressure measurements, and combustion chemical equilibrium simulations. A novel model of oxamide's effect on burn rate is also presented, and fits well to the experimental data. Finally, these propellant data and models are applied to select the propellant and chamber pressure for an example low-thrust solid rocket motor.

Nomenclature

a = Propellant burn rate coefficient [$\mathrm{m\,s^{-1}\,Pa^{-n}}$ or $\mathrm{mm\,s^{-1}\ MPa^{-n}}$]

A_b = Area of burning propellant surface [$\mathrm{m^2}$]

A_t = Nozzle throat area [$\mathrm{m^2}$]

c^* = Characteristic velocity of the propellant/motor [$\mathrm{m\,s^{-1}}$]

C_F = Thrust coefficient of the rocket motor [dimensionless]

F = Thrust force of the rocket motor [N]

h = Specific enthalpy [$\mathrm{J\,kg^{-1}}$]

I_{sp} = Specific impulse [s]

j = Mass flux [$\mathrm{kg\,m^{-2}\,s^{-1}}$]

$\dot{m}$ = Mass flow rate [$\mathrm{kg\,s^{-1}}$]

m_p = propellant grain mass [kg]

n = Propellant burn rate exponent [dimensionless]

*Graduate student, Department of Aeronautics and Astronautics, AIAA student member.
†Graduate student, Department of Aeronautics and Astronautics, AIAA student member.
‡T. Wilson Professor in Aeronautics, Department of Aeronautics and Astronautics, AIAA member

p_c = Chamber pressure of the motor [Pa]

q = Heat flux [$\mathrm{W\,m^{-2}}$]

r = Propellant burn rate [$\mathrm{m\,s^{-1}}$ or $\mathrm{mm\,s^{-1}}$]

w_{om} = Oxamide mass fraction [dimensionless]

γ = Combustion gas ratio of specific heats [dimensionless]

ϕ_{om} = Ratio of burn rate with oxamide / burn rate without oxamide [dimensionless]

λ = Burn rate model parameter [dimensionless]

ρ_s = Solid density of the propellant [$\mathrm{kg\,m^{-3}}$]

I. Introduction

A. Motivation: slow-burn propellants for low-thrust motors

Low-thrust, long-burn-time solid rocket motors may be useful as propulsion for small, fast uncrewed aerial vehicles (UAVs). These motors must deliver a low thrust level (just enough to counter drag) for a few minutes. Low thrust solid motors have also been examined for some in-space propulsion applications, where there is a requirement to limit the acceleration of the spacecraft to avoid structural damage [1, 2]. To achieve low thrust and long burn time, these motors use end-burn propellant grains, operate at low chamber pressure, and use slow-burn propellants. In many cases, it is desirable that the propellant burn rate should be adjustable (at the time of manufacture) so that similar propellants can serve a range of motor and mission concepts.

This paper describes the development of slow-burn ammonium perchlorate (AP) composite propellants which can operate in end-burn motors at low chamber pressure, and presents a novel model for oxamide's effect on burn rate in these propellants. The burn rate of these propellants can be adjusted by adding varying amounts of oxamide (a burn rate suppressant) to the propellant. The burn rate and other propellant properties are characterized as a function of oxamide content in this work. An accompanying paper [3] discusses the application of these propellants to low-thrust, long-burn-time motors for small, fast UAVs, and investigates other technology challenges of these motors.

The class of motors described in [3] have very low thrust relative to their size (e.g. kilogram-scale mass and 5–10 N of thrust, versus hundreds of newtons for typical kilogram-scale motors). This requires very low propellant burn rates of roughly 1–2 $\mathrm{mm\,s^{-1}}$. This is achieved by using a high oxamide content (up to 20% by mass) and very low chamber pressure (0.3–2 MPa). However, these propellants will not burn below a certain pressure; thus it is important to characterize the minimum burn pressure so that it can be imposed as a constraint on motor design.

B. Previous research on slow-burn propellants

AP composite propellants with oxamide are a known class of slow-burn propellants [4], and have been used in many low-thrust rocket motors (e.g. [2, 5, 6]). Although the effects of pressure and AP particle size on burn rate have been throughly studied (e.g. [7–9]), the effect of oxamide has received less attention, as slow-burn propellants are not widely used. Regarding the physical and chemical mechanisms of burn rate suppression, Trache et al. [10, 11] have provided some insight by investigating the thermal decomposition of oxamide-doped AP propellants and of pure oxamide. Burn rate data on specific propellants is somewhat scarce in the open literature, but some recent results have been published by Ghorpade *et al.* [12], Parhi *et al.* [13], and Jeenu *et al.* [14]. These works mostly considered oxamide contents of 4% or less, although [12] presents some data for a 10% oxamide propellant. None of these works have presented quantitative models for the effect of oxamide on burn rate.

C. Outline of this paper

Compared to previous works on slow-burn propellant, this work places greater emphasis on: 1) higher oxamide mass fractions, up to 20%, which give very slow burn rate coefficients; 2) testing and operation at low chamber pressures, and characterization of the minimum pressure at which the propellants can burn; and 3) models which allow oxamide content to be considered as a design variable at the preliminary design stage. First, the physical mechanisms by which propellant burn rate can be reduced are reviewed in section II. In section III, a new model is derived for the effect of oxamide on burn rate. Then, the effects of oxamide content on propellant properties are assessed, using chemical equilibrium simulations (section VI.A), strand burner experiments, and motor firings (sections V and VI). Finally, in section VII, these results are compared to burn rate data from other studies, and an example application of these results to rocket motor preliminary design is presented.

II. Techniques for reducing the propellant burn rate

Two techniques were used to create slow-burning AP composite propellants: large AP particles and a burn rate suppressant, oxamide. First, the propellant burn rate was decreased by increasing the AP particle size; however this effect saturates for particles larger than about 400 µm [9, 15], and using large AP particles alone does not make the propellant burn rate slow enough for this application.

To reduce the burn rate further, a burn rate suppressant was introduced as a minor ingredient in the propellant formulation. Burn rate tailoring is easily achieved by varying the amount of burn rate suppressant. Oxamide is the most notable of the burn rate suppressants, but others, including melamine, urea, and azodicarbonamide, are used [10, 12].

These burn rate suppressants act by absorbing heat at the burning surface of the propellant. At burning surface, suppressants decompose endothermically, and do so at a lower temperature than the other propellant ingredients [*]. This

[*]HTPB and AP decomposition data: [16–18], oxamide decomposition data: [10, 12].

cools the propellant surface, decreasing its decomposition rate.

III. Simple model for the effect of oxamide on burn rate

A simple, two-parameter model can characterize the propellant burn rate coefficient a as a function of the oxamide content w_{om}. The model is useful for fitting/interpolating $a(w_{om})$ between burn rates measured for different propellants. This model is derived by applying the conservation of energy and mass to a control volume containing the decomposing surface of the propellant. It assumes that the presence of oxamide 1) reduces the heat flux into the surface, by diluting and cooling the gas-phase flame and 2) increases the energy required to decompose a unit mass of solid propellant.

This theory predicts that the burn rate multiplier ϕ_{om} due to the addition of oxamide is:

$$\phi_{om} = \frac{1 - w_{om}}{1 + \lambda w_{om}} \tag{1}$$

where w_{om} is the mass fraction of oxamide in the propellant, and λ is a dimensionless parameter. λ can be predicted from thermochemical data, which suggest it is about 7 for typical AP composite propellants. The burn rate with oxamide is then $r_{om}(p_c) = \phi_{om}(w_{om})r_0(p_c)$, where $r_0(p_c)$ is the burn rate without oxamide.

In terms of the burn rate coefficient, a, the model is:

$$a = a_0 \frac{1 - w_{om}}{1 + \lambda w_{om}} \tag{2}$$

where a_0 is the burn rate coefficient with no oxamide. In practice, the parameters a_0, λ should be fit to experimental burn rate measurements. Fits to data are presented in section VI. It is assumed that the burn rate exponent n does not vary with oxamide content, an assumption that is supported by the data in section VI.

A. Derivation of the model

Begin by considering the application of the First Law of Thermodynamics to a control volume at the surface of the propellant (fig. 1). The control volume moves with the surface of the propellant as it regresses at a constant rate r. The control volume contains the surface reaction zone (and the gas-phase AP decomposition), but the main flame structure is outside of the control volume. Assume the flame is steady, so the mass and energy within the control volume do not change with time. A mass flux of solid propellant enters side 1 of the control volume:

$$j_1 = \frac{\dot{m}_s}{A_1} = \rho r \tag{3}$$

where A_1 is the area of side 1 and ρ_s is the density of the solid propellant. A mass flux of decomposed gas leaves side 2 of the control volume to supply the leading-edge and diffusion flames:

$$j_2 = -\frac{\dot{m}_g}{A_2} \tag{4}$$

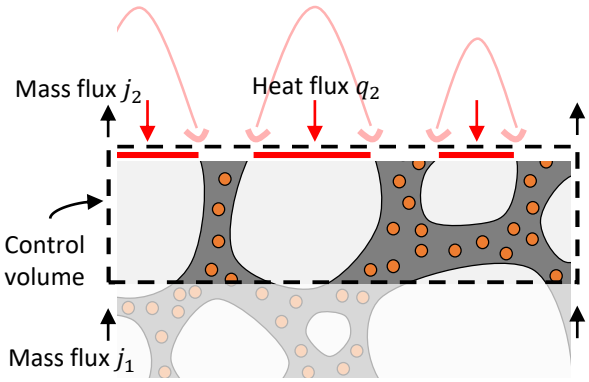

Fig. 1 The control volume, which moves with the propellant surface as it regresses.

By conservation of mass,

$$\frac{\mathrm{d}}{\mathrm{d}t}\int_{CV} \rho \, dV = 0 = j_1 + j_2 \tag{5}$$

Write the First Law for the control volume, assuming no mechanical work is done:

$$\frac{\mathrm{d}}{\mathrm{d}t} E_{CV} = \oint \vec{q} \cdot \vec{dA} + \oint \left(h + \frac{|v|^2}{2}\right) \vec{j} \cdot \vec{dA} \tag{6}$$

Now, make two assumptions to simplify the equation. First, assume that kinetic energy $\frac{|v|^2}{2}$ is negligible. Second, assume that the only relevant heat flux is q_2, from the flame to the surface; the conduction of heat deeper into the propellant, q_1, is negligible. The First Law becomes:

$$0 = -q_2 A_2 + j_1 h_1 A_1 + j_2 h_2 A_2 \tag{7}$$

where h_1 is the average specific enthalpy (thermal + chemical) of the solid entering at side 1, and h_2 is the average specific enthalpy of the gas leaving at side 2. Note that $A_1 = A_2$ (by definition) and $j_1 = -j_2$ (by conservation of mass), so the equation can be further simplified:

$$0 = -q_2 + \rho_s r (h_1 - h_2) \tag{8}$$

Solve for the burn rate r:

$$r = \frac{q_2}{\rho_s(h_1 - h_2)} \tag{9}$$

Define the surface gasification enthalpy, $\Delta h_{gas} = h_1 - h_2$:

$$r = \frac{q_2}{\rho_s \Delta h_{gas}} \tag{10}$$

This equation captures the dependence of the regression rate on the heat flux to the surface, and the energy required to gasify the surface. It is valid for endothermic surface decompositions with fast kinetics, where the rate of decomposition is limited primarily by the available energy. Exothermic surface decompositions (e.g. AP monopropellant) are not captured by this model; their regression rates depend on reaction kinetics, not on the rate of heat addition from an external flame.

Now, find the simplest possible expression for how each term in eq. (10) is influenced by the addition of oxamide.

Heat flux, q - Modeling the surface heat flux is complex. Rather than consider the details of this process, simply assume the heat flux is 'diluted' by a factor of $(1 - w_{om})$:

$$q = (1 - w_{om})q^* \tag{11}$$

Density ρ_s – The density of pure oxamide ($1670\,\mathrm{kg\,m^{-3}}$) and the density of the propellant ($1600\,\mathrm{kg\,m^{-3}}$) are approximately the same. Assume that adding oxamide does not affect the propellant density:

$$\rho_2 = \rho_s^* \tag{12}$$

Gasification enthalpy Δh_{gas} - The energy required to convert a unit mass of solid material at the initial temperature of side 1 to gaseous products just above the solid's decomposition temperature. Gasifying a unit mass of oxamide requires more energy than gasifying a unit mass of undoped propellant. The specific gasification enthalpy of a doped propellant is:

$$\Delta h_{gas} = \Delta h_{gas}^*(1 - w_{om}) + \Delta h_{gas}^{om} w_{om} \tag{13}$$

where Δh_{gas}^* is the specific gasification enthalpy of undoped propellant, and Δh_{gas}^{om} is the specific gasification enthalpy of pure oxamide. This model assumes that propellant and oxamide gasify separately, i.e. the oxamide has no catalytic or inhibitory effect on the propellant's gasification reactions. To simplify the above equation, the parameter λ is introduced:

$$\Delta h_{gas} = (1 + \lambda w_{om})\Delta h_{gas}^* \tag{14}$$

where:

$$\lambda \equiv \frac{\Delta h_{gas}^{om} - \Delta h_{gas}^{*}}{\Delta h_{gas}^{*}} \tag{15}$$

Substitute each of these relations into eq. (10):

$$r = \frac{q_2}{\rho_s \Delta h_{gas}} = \frac{(1 - w_{om}) q_2^{*}}{(1 + \lambda w_{om}) \rho_s^{*} \Delta h_{gas}^{*}} = \frac{1 - w_{om}}{1 + \lambda w_{om}} r^{*} \tag{16}$$

Therefore,

$$\phi(w_{om}) = \frac{1 - w_{om}}{1 + \lambda w_{om}} \quad \blacksquare \tag{17}$$

IV. Composition of the slow-burn propellants

The effect of oxamide on burn rate was investigated by mixing and testing propellants with oxamide mass fractions of 0%, 5%, 10%, 13% and 20%. The burn rate is reduced by a factor of four over this range of oxamide content. These propellants are based on a standard ammonium perchlorate composite propellant with no metal fuel. The "base" propellant consists of 80% AP and 20% HTPB-based binder; its composition is listed in table 1. To make a propellant with w_{om} oxamide mass fraction, all the ingredient mass fractions in table 1 were multiplied by $(1 - w_{om})$, and w_{om} of oxamide was added.

Two AP particle size distributions were used in this work: a '400/200 micron blend' of 400 µm diameter rounded particles, 200 µm diameter rounded particles, and finer ground particles; and a '400 micron blend' of 400 µm diameter rounded particles and finer ground particles. The use of large (400 µm) AP particles reduces the propellant burn rate. A blend including finer ground particles enables higher solids loading and makes the propellant more castable [4, 19]. Propellants with 0%, 10% and 13% oxamide were made with the '400/200 micron blend' AP. Propellants with 5% and 20% oxamide were made with the '400 micron blend' AP. Both AP blends were coated with tricalcium phosphate (anti-caking agent) by the manufacturer [†].

The binder was primarily hydroxyl-terminated polybutadiene (HTPB). The HTPB resin had a molar mass of 2800 g mol^{-1}. It was cross linked with Modified MDI (a diphenyl methane diisocyanate). The HTPB resin was purchased pre-mixed with CAO-5 (anti-oxidant) and HX752 (bonding agent). Isodecyl pelargonate (IDP, plasticizer), and graphite powder (opacifier) were added to the binder [‡]. The 0%, 5%, 10% and 13% oxamide propellant formulations used 2.20% carbon powder, which was later determined to be an excessively high amount. For the 20% oxamide propellant, the carbon powder mass fraction was reduced to 0.20%, with the balance replaced by HTPB resin and

[†]The AP blends were purchased from RCS Rocket Motor Components, Inc. of Cedar City, Utah.

[‡]All of the binder chemicals, except the graphite powder, were purchased from RCS Rocket Motor Components, Inc.

Table 1 The 0% oxamide propellant. Other propellants mixed $(1-w_{om})$ of these ingredients with w_{om} oxamide.

	Purpose	Ingredient	Mass fraction [%]
Binder			20.00
	Resin	Hydroxyl-terminated polybutadiene	10.98
	Binding agent	HX-752	0.27
	Anti-oxidant	CAO-5	0.11
	Curative	Modified MDI	1.72
	Plasticizer	Isodecyl pelargonate	4.72
	Opacifier	Carbon powder	2.20
Oxidizer			80.00
		Ammonium perchlorate	80.00

curative in the same ratio as in table 1. The authors recommend this for future works with these propellants.

V. Methods for propellant characterization

A. Propellant mixing and casting

The propellant was mixed in a custom vacuum mixer [§] in order to remove water and other volatiles from the propellant precursors and prevent air from being mixed into the propellant during mixing. All ingredients except the curative were gradually incorporated, then the propellant was mixed under vacuum for two hours at a mixer speed of 25 rpm. Finally, the curative was added while maintaining vacuum (through a valve in the mixer lid), and the propellant was mixed for another 10 minutes. Further descriptions of the vacuum mixer and propellant mixing procedures can be found in [20]. After the propellant was mixed, it was either cast into sample tubes for strand burner tests or into molds for a research motor. The as-cast propellant densities were between 1540–1570 $\mathrm{kg\,m^{-3}}$ (95.6–97.5% of the theoretical density of 1610 $\mathrm{kg\,m^{-3}}$). These configurations are described further in the following sections.

B. Strand burner apparatus

A set of burn rate measurements were performed in a strand burner, which burns small samples ("strands") of solid propellant at a controlled pressure. Several samples of each propellant were burned at different pressures; this process was repeated for 5 different propellants (0%, 5%, 10%, 13% and 20% oxamide content). These data allow insight into how the burn rate varies with both pressure and oxamide content.

When propellant batches were mixed, propellant samples were taken for testing in the strand burner. The samples of propellant were cast into glass tubes (9.7 mm ID x 90.5 mm long). After filling, the propellant was left to cure in the tubes.

Each propellant-filled sample tube was connected to a pressurized plenum. The plenum pressure was controlled by a

[§] A heavily modified Bosch MUM6N10 Universal Plus Mixer with a 6 L capacity was used.

regulator providing argon gas to the plenum at the set test pressure, and by a backpressure regulator venting excess gases from combustion. The propellant was ignited by a small (0.1 g) piece of starter propellant[¶], which was itself ignited by a 6 W blue laser. Figure 2 shows a sequence of video frames of a burning propellant sample. The first frame shows a blue/purple glow from the laser light igniting the starter propellant. The subsequent frames show the flame front progressing along the strand. Additional details of the strand burner design are presented in [21].

The burn rate was measured by video, and the pressure was recorded with a pressure transducer. The time to burn the propellant sample was determined via a frame-by-frame review of the video. Although ignition and burnout of the propellant did not occur instantly, the times of those events were clearly discernible to within 0.04 s (10 video frames at 250 frames per second). The length of each propellant strand was measured with calipers to an accuracy of 1 mm. The plenum pressure was measured with a Omega PX119-600AI pressure transducer with a rated accuracy of 0.02 MPa.

For each propellant formulation, several (4 to 10) strands were burned at different pressures, and their burn rates determined. Then, the burn rate parameters a and n were fit to these (pressure, burn rate) points using a non-linear least squares algorithm[‖]. Additionally, 95% confidence intervals were determined for the a and n values using the F-test method.

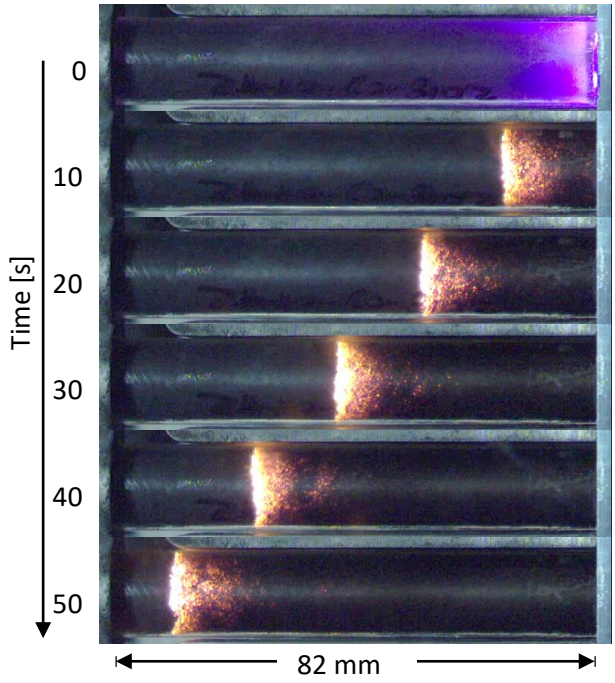

Fig. 2 Video frames from burning a strand of 13% oxamide propellant at a pressure of 0.52 MPa. The propellant burn rate was measured to be 1.42 mm s^{-1}.

[¶]Cesaroni Technologies 'Classic' propellant.
[‖]The `lmfit` python package was used to perform the fits.

C. Research motor

Several propellants were also test-fired in a research motor, to confirm their stable combustion at low chamber pressures and to measure the burn rate under more realistic conditions (typically, burn rates are slightly lower in a strand burner than in a motor).

The research motor's components are shown in fig. 3. The motor case is a round tube made from grade 2 titanium. The case contains an ablative liner and the propellant grain. The end-burning propellant grain burns from right to left in fig. 3. The ablative liner protects the motor case from the hot combustion gases.

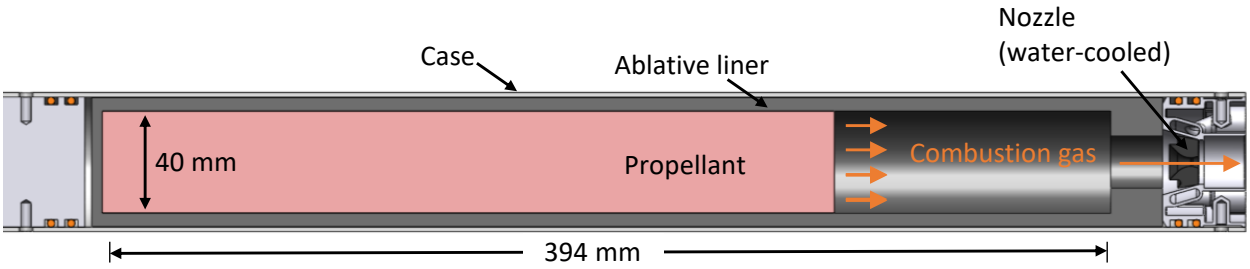

Fig. 3 Cross section of the research motor, showing the end-burn propellant grain, ablative liner, and water-cooled nozzle.

The motor uses an end-burn propellant grain, which is 40 mm in diameter. A full-length propellant grain has a mass of about 700 g, although sometimes the motor has been tested with shorter-length propellant grains.

To facilitate ignition, a 'starter pocket' is cast into the aft face of the propellant grain. It was found that a flat face of slow-burn propellant could not be reliably ignited. Ignition was made more reliable by placing a small (2–4 g) piece of faster-burning propellant ('starter grain') into a 'starter pocket' in the aft end of the propellant grain. The starter grain was ignited by a 6 W blue laser shone through the nozzle. The burning starter grain then ignited the main propellant grain around it. The additional burn area of the starter pocket causes an initial peak in chamber pressure. After the starter pocket burns away, the burning surface becomes a flat circle (with burn area $\pi(20\,\text{mm})^2 = 1257\,\text{mm}^2$) and the chamber pressure levels off at a lower value for the rest of the firing.

Before loading into the motor, the mass of each propellant grain was measured with an accuracy of 1 g. The chamber pressure was measured with a Omega PX119-600AI pressure transducer with a rated accuracy of 0.02 MPa. Further details on the motor instrumentation and its accuracy are presented in [3, 21].

Because the chamber pressure was not constant, estimating burn rate from the motor firings is somewhat involved. Two techniques were used: a 'average burn rate method' and a 'c^*-based method'; these methods are described in [21], appendix A. The accuracy of these burn rate estimation methods has not been rigorously calibrated, but a propagation of error analysis following [22] estimates errors of 3% and 7% for each method, respectively. The burn rates estimated by the two methods sometimes differ by up to 15%.

VI. Propellant characterization results: experiment and simulation

A. Predicted performance from combustion simulation

Combustion simulations (chemical equilibrium calculations [**]) were performed on this family of propellants to predict how the properties of the combustion gas would vary with oxamide content. Figure 4 shows the variation in ideal flame temperature and characteristic velocity. As expected, the flame temperature and characteristic velocity decrease when more oxamide is added to the propellant. However, the decrease in c^* is much smaller than the decrease in burn rate. Adding 20% oxamide decreases the burn rate by 75%, but only decreases c^* by 16%. Also, adding oxamide causes minor variations in the combustion gas ratio of specific heats (γ) and the solid propellant density (ρ_s). These are not large enough to be important to motor performance.

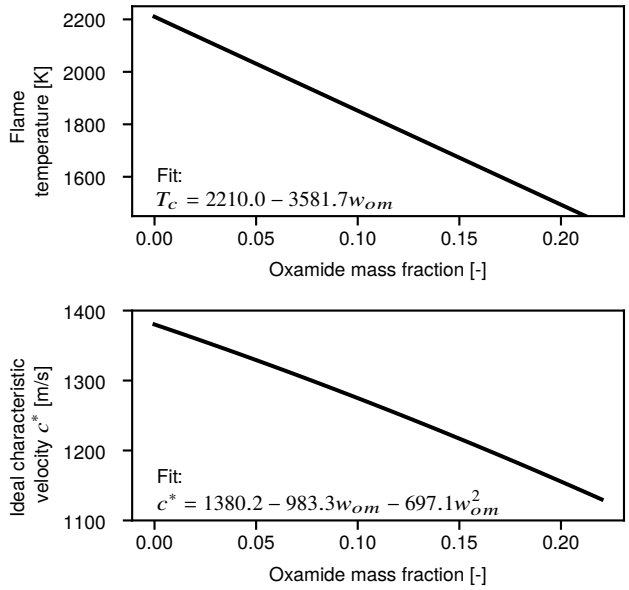

Fig. 4 Chemical equilibrium simulation results for the ideal flame temperature and characteristic velocity of the propellant.

B. Burn rate in the strand burner

The burn rate vs. pressure measurements from the strand burner are presented in fig. 5. Each propellant formulation is shown in a different color. For AP particle size, the 0%, 10% and 13% oxamide propellants used the '400/200 micron blend'. The 5% and 20% oxamide propellants used the '400 micron blend' and thus had a larger average AP particle size. Each point is the burn rate and pressure for a particular strand burner sample. The horizontal error bars show how much the strand burner pressure varied during the burn [††]. Error bars on burn rate are too small to be visible in this plot.

[**]Using the *Rocket Propulsion Analysis* (RPA) combustion equilibrium software published by Rocket Propulsion Software+Engineering UG, Neunkirchen-Seelscheid, Germany

[††]The pressure control system had some dead-band, so the pressure in the strand burner varied slightly while each sample burned.

For the 20% oxamide propellant, the combination of low flame temperature and small strand size caused the samples to not burn well in the strand burner at pressures above 1.2 MPa. At higher pressures, more heat was lost by convection to the sample tubes, causing the flame to self-extinguish a few seconds after ignition. All other propellants burned well at the highest pressure for which each was tested.

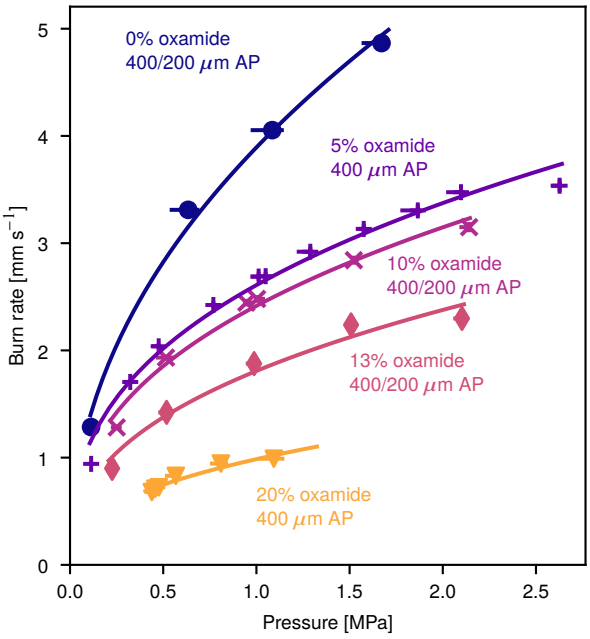

Fig. 5 Strand burner experiments measured the burn rate of each propellant at several pressures. A Vieille model ($r = ap^n$) was fit to the measurements from each propellant.

The standard burn rate fitting method is Vieille's formula, $r = ap^n$, with a and n as free parameters. A separate $r = ap^n$ fit was performed for each propellant (curves in fig. 5). Within each propellant, the burn rate is higher at higher pressures. Between propellants, propellants with more oxamide burn more slowly at a given pressure.

The a, n values from each propellant are plotted in fig. 6. The fit values of a and n are shown as colored points, and the 95% confidence intervals from the Vieille fit are shown with error bars. As expected, the burn rate coefficient a is lower for propellants with more oxamide.

The model of $a(w_{om})$ (eq. (2)) was fit to these points. Two different fits were made for the two different AP particle sizes: '400/200 micron blend' and '400 micron blend'. The fits were allowed to have different a_0 values, but constrained to have the same λ value. A nonlinear least squares method[‡‡] was used to solve the fits. In the top subplot of fig. 6, the $a(w_{om})$ model for the '400/200 micron blend' AP is shown as a solid curve, and the model for the '400 micron blend' AP is shown as a dashed curve. Each point is connected to its model by a gray line. The burn rate coefficient is lower for the propellants with '400 micron blend' AP because larger AP particles reduce the burn rate.

[‡‡]Implemented in the python package `lmfit`.

The burn rate exponent n is shown in the bottom plot of fig. 6. n does not show significant variations with oxamide content. For all propellants, the error bars on n overlap with the mean value of $n = 0.402$.

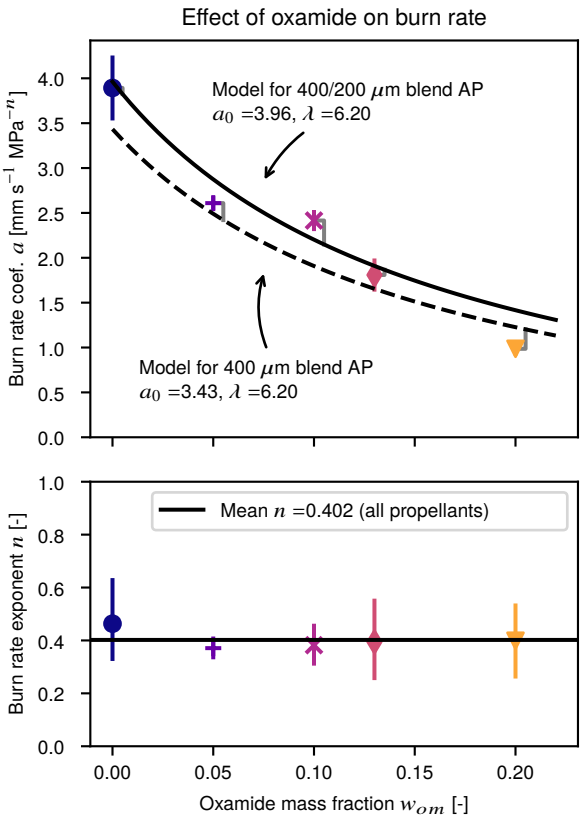

Fig. 6 The burn rate coefficient a decreases with oxamide content, whereas the exponent n is roughly constant. a, n values are from the curve fits in fig. 5; error bars show 95% confidence interval.

C. Minimum burn pressure

For each propellant, there is a minimum pressure below which it will not burn. This sets a lower limit on the chamber pressure and propellant burn rate at which the motor can operate. Low thrust, long burn time motors require low chamber pressure and slow propellant burn rate, so it is important to know this lower limit. It is not possible to predict the minimum burn pressure from first principles, so experimental characterization is necessary.

The minimum burn pressure was investigated with the strand burner (fig. 7). For each propellant formulation, we do not know the minimum burn pressure exactly, but do have lower and upper limits from the strand burner. The lower limit is the highest pressure at which a strand burner sample would not burn. The upper limit is the lowest pressure at which a strand burner sample ignited and burned. In these strand burner experiments, we first attempted to ignite each formulation at atmospheric pressure (0.1 MPa). If the sample did not ignite, we then attempted to ignite it incrementally higher pressures until it did ignite. The 0 and 5% oxamide propellants burned at atmospheric pressure. The 10% and

13% oxamide propellants did not burn at atmospheric pressure but did burn at 0.2 MPa. The 20% oxamide propellants did not burn until the pressure was raised to 0.4 MPa. A simple quadratic fit (black line) is shown with the data. This fit should be regarded with some skepticism as there is no theoretical basis for the relationship to be quadratic, and the fit is based on a small number of tests.

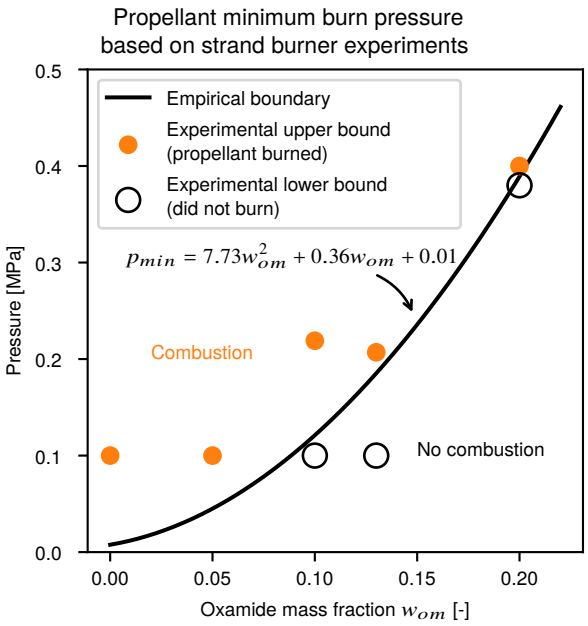

Fig. 7 The minimum burn pressure is the minimum pressure at which the propellant will sustain combustion; it increases with oxamide content.

D. Burn rate in the research motor

The burn rate was also estimated from the research motor firings. Results are presented for five static firings of the motor, which are designated SF-A, SF-B, SF-C, SF-D and SF-E. The motor firings and research motor are describe further in [3].

It is important to compare the strand burner burn rates to burn rates measured in a representative motor, as the burn rate is usually slightly faster in a motor [4, 23]. As an example, the burn rate data for the 13% oxamide propellant are shown in fig. 8; measurements from the motor are indicated with black 'x' and '+' marks, measurements from the strand burner are shown in pink. Note that the motor burn rate is slightly higher than the strand burner Vieille fit (pink curve) would predict. Across all the tested propellants, burn rates measured in the motor are consistently higher than those measured in the strand burner. On average, the motor burn rates were 19% higher than the strand burner fits would predict.

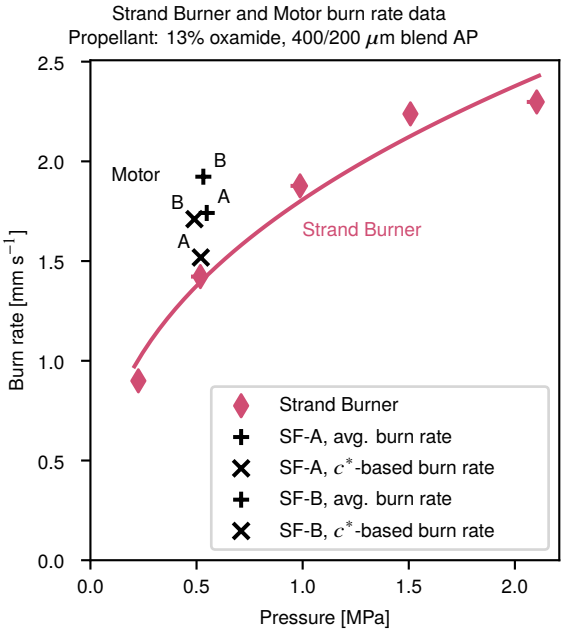

Fig. 8 Burn rate data from the research motor (black '+' and 'x' marks) and strand burner (pink curve and points) for the 13% oxamide propellant. The propellant burns faster in the motor than in the strand burner.

The propellant burn rate coefficient vs. oxamide content is shown in fig. 9. The motor firing burn rate measurements are shown as '+' and '×' marks[§§]. The oxamide model (curves) fits the motor firing data well. The fit curves for the motor firings are 19% higher than that those for the strand burner in fig. 6. The oxamide model as fit to the motor firings in fig. 9 should be used for motor preliminary design. Some motor firings used propellants with different AP particle size blends; propellants with the '400 micron blend' AP particle size burn more slowly, and their burn rates are better predicted by evaluating the model (eq. (2)) with a lower a_0 value.

Some unburnt propellant residue was left at the end of the motor firings. The residue appeared to be carbon-based soot, and was about 1-2% of the initial mass of the propellant. These propellants contained an excessive amount of carbon powder opacifier, and this may have contributed to the residue.

E. Operation at low chamber pressure and low thrust

Stable motor operation at very low thrust and chamber pressure was achieved in static fires SF-A and B. Both firings used a 13% oxamide propellant; the 'steady' chamber pressure was 0.52 MPa in SF-A and 0.49 MPa in SF-B. Static fire SF-E, using 20% oxamide propellant, burned stably for 54 s, but then self-extinguished before burning all of the available propellant. The chamber pressure gradually declined while the propellant was burning, likely due to a combination of nozzle erosion and increasing heat loss through the motor walls as the propellant grain receded. The propellant self-extinguished when the chamber pressure had decreased to approximately 0.5 MPa, near the minimum

[§§] More motor firing data, including pressure and thrust traces for each firing, are available in [3, 21].

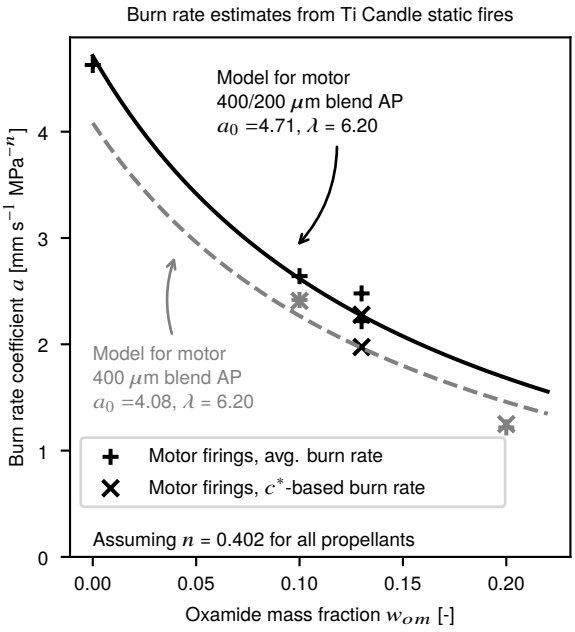

Fig. 9 The oxamide model is also a good fit for burn rate vs. oxamide measurements from motor firings. The baseline burn rate coefficient a_0 for the motor is 1.19 times that for the Strand Burner.

burning pressure for 20% oxamide propellant shown in fig. 7.

Demonstrating operation at low chamber pressure, close to the minimum burn pressure of the propellant, is an important validation, as some other propellants and motors exhibit low-frequency combustion instability (chuffing) when operated at low chamber pressure [4]. These tests show that this slow-burn propellant can operate at very low p_c without chuffing, which is necessary for low-thrust motors.

F. Characteristic velocity measurements

The time-averaged c^* was measured from the pressure recording $p_c(t)$, the nozzle throat area A_t, and the propellant grain mass m_p:

$$\langle c^* \rangle = \frac{A_t}{m_p} \int_{t_{start}}^{t_{end}} p_c(t) dt \tag{18}$$

The characteristic velocity measured in the motor firings was 83-96% of the propellant's ideal c^* (as calculated by chemical equilibrium simulations). Because of the motor's small size, end-burn grain and low mass flow rate, the combustion gas was cooled significantly by heat loss to the chamber walls before reaching the nozzle inlet. As c^* is proportional to the square root of gas stagnation temperature at the nozzle inlet, this heat loss reduced c^*. Detailed calculations of the heat loss are presented in [21] and are consistent with a c^* efficiency of about 85%.

VII. Discussion

A. Comparison to other studies of the effect of oxamide on burn rate

The effect of oxamide on burn rate measured in this work agrees with measurements from other studies [6, 10, 12–14]. A comparison is shown in fig. 10. Data from this work are shown in blue; other studies in black. To compare burn rate data from different studies, which used different baseline propellants, the burn rate data are shown in terms of the burn rate multiplier ϕ_{om}. ϕ_{om} is the ratio of the propellant burn rate with oxamide to the burn rate of that study's baseline, no-oxamide propellant (at the same pressure).

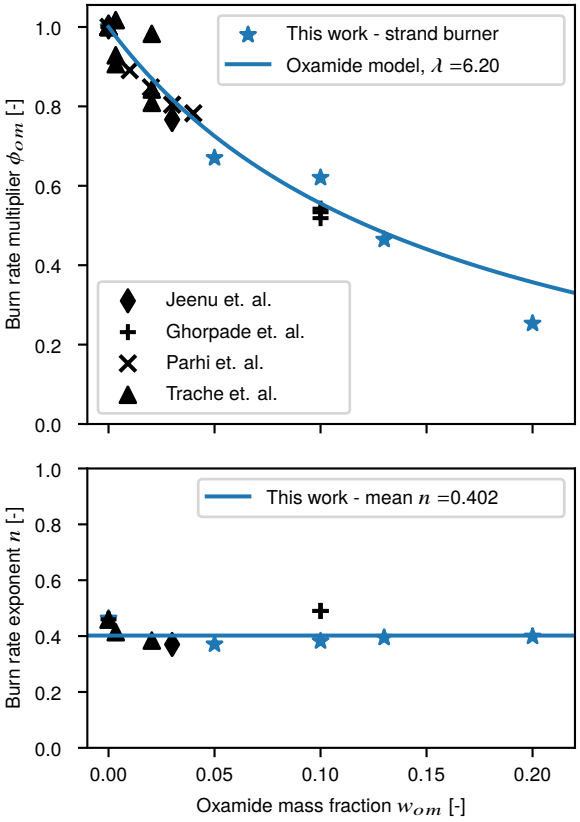

Fig. 10 Various assessments of the effect of oxamide on propellant burn rate. The oxamide model (blue curve) and strand burner data (blue stars) from this work agree with measurements from other studies (black marks).

Despite the various propellant formulations and test pressures, all the ϕ_{om} data cluster around the oxamide model presented in this work. All of the burn rate exponent data clusters around $n = 0.4$. As shown in fig. 10, the burn rate data has now been extended to higher oxamide contents. The highest oxamide content reported in the previous literature was 10%; at this oxamide content, the burn rate was halved ($\phi_{om} = 0.5$). Most studies used oxamide contents less than 5%. The experimental data from this work extends to an oxamide mass fraction of 20%, which reduces the burn rate to roughly $\phi_{om} = 0.3$. As will be discussed in section VII.B, the data now cover the range of oxamide contents which are

likely to be useful for low-thrust long-burn time motors.

B. Application of propellant data to preliminary design of low-thrust, long-burn-time motors

Slow-burn propellants are useful for motors with low thrust relative to their size; this can be quantified by the (thrust / burn area) ratio, F/A_b. As discussed in [3], typical AP-propellant motors operate at F/A_b of 15–35 kPa, whereas 'low-thrust' motors have lower F/A_b. For small, fast aircraft motors, the required F/A_b is set by the cruise speed, altitude, and aerodynamic design, and may be as low as 3 kPa. The propellant data presented above can be used to select a propellant composition and chamber pressure for a motor with a given F/A_b requirement. This analysis will determine the p_c and propellant oxamide content which maximizes the motor's specific impulse, while meeting the F/A_b requirement.

The results are computed over a sweep of oxamide contents. For each oxamide content, a is evaluated from eq. (2) with $a_0 = 4.08\,\mathrm{mm\,s^{-1}\,MPa^{-n}}$, $\lambda = 6.20$ (representative of propellants with the '400 µm blend' AP in motor conditions), and ρ_s, c^*, γ are looked up from chemical equilibrium simulation results. Then, p_c is found by solving:

$$\frac{F}{A_b} = p_c^n C_F(p_c, p_e, p_a, \gamma) c^* a \rho_s \tag{19}$$

$C_F(p_c, p_e, p_a, \gamma)$ is computed using the ideal 1-dimensional channel flow model from [4], chapter 3. Specific impulse is $I_{sp} = C_F c^*/g_0$. Note that this analysis assumes ideal performance. In a real motor, inefficiencies in the nozzle and combustion will reduce C_F and c^* below their ideal values.

The results are shown in fig. 11. Each colored curve is for a different value of F/A_b. Oxamide contents and chamber pressures in the gray shaded region are not feasible – the chamber pressure is so low that either the nozzle would not choke or the propellant would not burn. The $F/A_b = 3$ kPa curve approaches this lower limit. F/A_b ratios as low as 2.4 kPa have been demonstrated in motor firings. F/A_b ratios below 2 kPa are not feasible with these propellants at any oxamide content.

For a given F/A_b, there is an oxamide content which maximizes I_{sp} (marked with '★'s). This is due to opposite trends in C_F and c^* with increasing oxamide content. Higher oxamide content allows higher p_c while keeping a low burn rate, and higher p_c improves C_F. However, adding more oxamide to the propellant reduces the flame temperature, which reduces c^*. The first effect becomes less important as p_c increases.

For each F/A_b curve, a wide range of oxamide contents around the maximum give only small changes in I_{sp}. A practical choice of propellant will consider other factors, not just I_{sp}. Propellants with higher oxamide contents are more difficult to ignite and have higher solids loading (more difficult to mix), and lower chamber pressure reduces heat transfer to the motor components. These considerations could motivate using a w_{om} somewhat below the I_{sp}-maximizing value. Oxamide contents above 20% do not improve I_{sp} much, and would be difficult to ignite and difficult to mix. This

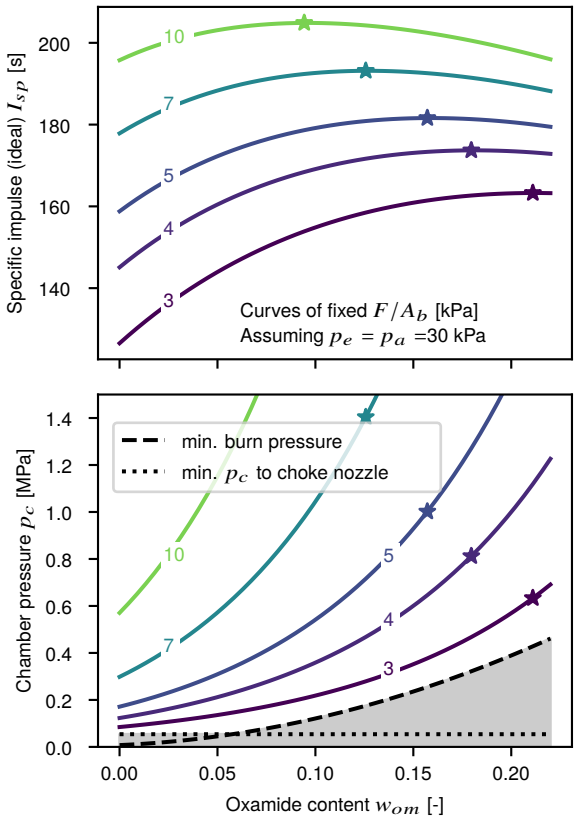

Fig. 11 Specific impulse and chamber pressure vs. oxamide content, for different F/A_b ratios. The curves were computed by solving eq. (19) using propellant data from sections VI and VI.A.

indicates that the experiments in this work, which tested oxamide contents from 0-20%, have covered the useful range of oxamide contents for the low-thrust motor application.

VIII. Conclusion

Low-thrust, long-burn-time solid rocket motors require slow-burn propellant. This work developed slow-burn propellants and a new model to quantify how the burn rate is reduced by adding oxamide to the propellant. These slow-burn ammonium perchlorate composite propellants employ two known techniques to reduce the burn rate: large AP particles and the burn rate suppressant oxamide. The propellant's burn rate is adjustable (at the time of manufacture), so that a set of similar propellants can accommodate a range of missions and aircraft concepts. The burn rate is adjusted by varying the oxamide content; propellants with oxamide contents of 0 to 20% were tested, with burn rate decreasing by a factor of 4 over this range (burn rate coefficient a from 4.7 mm s^{-1} MPa^{-n} to 1.5 mm s^{-1} MPa^{-n}). The oxamide/burn rate model fits the experimental data well.

Oxamide has been known as a burn rate suppressant for some time. The experimental results presented here extend previous studies on oxamide to higher oxamide contents (up to 20%). Burn rates were measured at low pressures relevant

to low-thrust motors, and the minimum burn pressure was measured as a function of oxamide content. Previous studies were mostly conducted at higher pressures, and did not measure the minimum burn pressure. These measurements are important because low thrust motors operate at unusually low chamber pressure (0.3–2 MPa). Further, it was demonstrated that these propellants can operate in a small motor at these low chamber pressures without chuffing instabilities.

These results demonstrate a feasible set of propellants for the low-thrust, long-burn-time motors described in [3]. The motor given as a motivating example ($\sim$ 10 N thrust with a $\sim$ 60 mm diameter end-burning propellant grain) requires a propellant burn rate of 1–2 mm s^{-1}, which these propellants can provide. The propellant data and models presented here will be useful to the design and development of such motors, and to other applications which require slow-burn solid propellants.

Funding Sources

This work was funded by BAE Systems, Inc., MIT Lincoln Laboratories and the US Department of Defense's Rapid Reaction Technology Office (RRTO).

Acknowledgments

Several undergraduate researcher assistants contributed to the propellant work, particularly Carlos ('Charlie') Garcia, who first suggested the use of oxamide-inhibited AP composite propellant, and Katya Bezugla, who performed the chemical equilibrium software runs.

References

[1] Shafer, J. I., "Solid-Propellant Motors for High-Incremental-Velocity Low-Acceleration Maneuvers in Space," JPL-TM-33-528, Jet Propulsion Laboratory, Pasadena, California, Mar. 1972.
https://ntrs.nasa.gov/search.jsp?R=19720012197.

[2] Nowakowski, P., Kasztankiewicz, A., Marciniak, B., Okninski, A., Pakosz, M., Noga, T., Majewska, E., Rysak, D., and Wolanski, P., "Space Debris Mitigation Using Dedicated Solid Rocket Motor," *8th European Conference for Aeronautics and Space Sciences*, Madrid, Spain, 2019.
https:/doi.org/10.13009/EUCASS2019-994.

[3] Vernacchia, M. T., Mathesius, K. J., and Hansman, R. J., "Low Thrust Solid Rocket Motors for Small, Fast Aircraft Propulsion," *Journal of Propulsion and Power (not yet published)*,

[4] Sutton, G. P. and Biblarz, O., *Rocket Propulsion Elements*, 8th ed. John Wiley & Sons, Inc., Hoboken, New Jersey, 2010.

[5] Compton, J., Thies, C., Kurzeja, S., and McGarry, J., "Five-Minute Rocket Motor," *AIAA/SAE 10th Propulsion Conference*, AIAA, San Diego, California, Oct. 1974.
https://doi.org/10.2514/6.1974-1203.

[6] Parhi, A., Mahesh, V., Kalluru, K., Reshmi, S., Harikrishnan, R., Lakshmi, V. M., Murugan, J. P., and Reddy, R. K., "Development of Slow-Burning Solid Rocket Booster for RLV-TD Hypersonic Experiment," *Current Science*, Vol. 114, No. 1, 2018, pp. 74–83.
https://doi.org/10.18520/cs/v114/i01/74-83.

[7] Ramohalli, K., "Steady-State Burning of Composite Propellants under Zero Cross-Flow Situation," *Fundamentals of Solid-Propellant Combustion*, edited by K. Kuo and M. Summerfield, Vol. 90, Progress in Astronautics and Aeronautics, AIAA, New York, 1984, pp. 409–477.
https://doi.org/10.2514/5.9781600865671.0409.0477.

[8] Cohen, N. S., "Review of Composite Propellant Burn Rate Modeling," *AIAA Journal*, Vol. 18, No. 3, 1980, pp. 277–293.
https://doi.org/10.2514/3.50761.

[9] Gross, M. L. and Beckstead, M. W., "Steady-State Combustion Mechanisms of Ammonium Perchlorate Composite Propellants," *Journal of Propulsion and Power*, Vol. 27, No. 5, 2011, pp. 1064–1078.
https://doi.org/10.2514/1.B34053.

[10] Trache, D., Maggi, F., Palmucci, I., DeLuca, L. T., Khimeche, K., Fassina, M., Dossi, S., and Colombo, G., "Effect of Amide-Based Compounds on the Combustion Characteristics of Composite Solid Rocket Propellants," *Arabian Journal of Chemistry*, Dec. 2015.
https://doi.org/10.1016/j.arabjc.2015.11.016.

[11] Trache, D., Maggi, F., Palmucci, I., and DeLuca, L. T., "Thermal Behavior and Decomposition Kinetics of Composite Solid Propellants in the Presence of Amide Burning Rate Suppressants," *Journal of Thermal Analysis and Calorimetry*, Vol. 132, No. 3, 2018, pp. 1601–1615.
https://doi.org/10.1007/s10973-018-7160-8.

[12] Ghorpade, V. G., Dey, A., Jawale, L. S., Kotbagi, A. M., Kumar, A., and Gupta, M., "Study of Burn Rate Suppressants in AP-Based Composite Propellants," *Propellants, Explosives, Pyrotechnics*, Vol. 35, No. 1, 2010, pp. 53–56.
https://doi.org/10.1002/prep.200800046.

[13] Parhi, A., Mahesh, V., Shaji, A., Levin, G., Abraham, P. J., and Srinivasan, V., "Challenges in the Development of a Slow Burning Solid Rocket Booster," *Aerospace Science and Technology*, Vol. 43, Jun. 2015, pp. 437–444.
https://doi.org/10.1016/j.ast.2015.04.001.

[14] Jeenu, R., Pinumalla, K., and Deepak, D., "Industrial Adaptation of Ultrasonic Technique of Propellant Burning Rate Measurement Using Specimens," *Journal of Propulsion and Power*, Vol. 29, No. 1, 2013, pp. 216–226.
https://doi.org/10.2514/1.B34578.

[15] Thomas, J. C., Morrow, G. R., Dillier, C. A. M., and Petersen, E. L., "Comprehensive Study of Ammonium Perchlorate Particle Size/Concentration Effects on Propellant Combustion," *Journal of Propulsion and Power*, Vol. 36, No. 1, 2019, pp. 95–100.
https://doi.org/10.2514/1.B37485.

[16] Arisawa, H. and Brill, T. B., "Flash pyrolysis of hydroxyl-terminated polybutadiene (HTPB) I: Analysis and implications of the gaseous products," *Combustion and Flame*, Vol. 106, No. 1, 1996, pp. 131–143.
http://www.sciencedirect.com/science/article/pii/0010218096002532.

[17] Tingfa, D., "Thermal Decomposition Studies of Solid Propellant Binder HTPB," *Thermochemical Acta*, Vol. 138, No. 2, 1989, pp. 189–197.
https://doi.org/10.1016/0040-6031(89)87255-7.

[18] Kubota, N., *Propellants and Explosives: Thermochemical Aspects of Combustion*. John Wiley & Sons, Inc., Hoboken, NJ, 2015.

[19] Davenas, A., *Solid Rocket Propulsion Technology*. Pergamon Press, New York, 1993.
https://doi.org/10.1016/C2009-0-14818-3.

[20] Mathesius, K. J., "Manufacturing Methods for a Solid Rocket Motor Propelling a Small, Fast Flight Vehicle," MS thesis, Massachusetts Institute of Technology, Cambridge, Massachusetts, Jun. 2019.
https://dspace.mit.edu/handle/1721.1/122377.

[21] Vernacchia, M. T., "Development of Low-Thrust Solid Rocket Motors for Small, Fast Aircraft Propulsion," Ph.D. Dissertation, Massachusetts Institute of Technology, Cambridge, Massachusetts, May 2020.
https://hdl.handle.net/1721.1/127069.

[22] "Propagation of Error for Many Variables," *NIST/SEMATECH e-Handbook of Statistical Methods*, National Institute of Standards and Technology, Gaithersburg, Maryland, Oct. 2013.
https://doi.org/10.18434/M32189.

[23] Blair, D. W., "The Influence of Diameter on the Burning Velocity of Strands of Solid Propellant," *Combustion and Flame*, Vol. 20, No. 1, 1973, pp. 105–109.
https://doi.org/10.1016/S0010-2180(73)81261-1.